Title

Choroidal Changes in Rhesus Macaques in Aging and Age-Related Drusen

Journal

Investigative Ophthalmology & Visual Science, 64(12)

ISSN

0146-0404

Authors

Sazhnyev, Yevgeniy

Sin, Tzu-Ni

Ma, Anthony

et al.

Publication Date

2023-09-29

DOI

10.1167/iovs.64.12.44

Peer reviewed

Choroidal Changes in Rhesus Macaques in Aging and Age-Related Drusen

Yevgeniy Sazhnyev,[1,2] Tzu-Ni Sin,[1] Anthony Ma,[1,2] Ellie Chang,[1] Leon Huynh,[1] Karolina Roszak,[1] Sangwan Park,[1] Kevin Choy,[3] Sina Farsiu,[3,4] Ala Moshiri,[1] Sara M. Thomasy,[1] and Glenn Yiu[1]

[1]Department of Ophthalmology & Vision Science, University of California, Davis, Sacramento, California, United States
[2]Department of Ophthalmology, California Northstate University, College of Medicine, Elk Grove, California, United States
[3]Department of Biomedical Engineering, Duke University, Durham, North Carolina, United States
[4]Department of Ophthalmology, Duke University Medical Center, Durham, North Carolina, United States

Correspondence: Glenn Yiu, Department of Ophthalmology & Vision Science, University of California, Davis, 4860 Y St., Suite 2400, Sacramento, CA 95817, USA; gyiu@ucdavis.edu.

YS and TNS contributed equally to this study.

Received: April 13, 2023
Accepted: September 7, 2023
Published: September 29, 2023

Citation: Sazhnyev Y, Sin TN, Ma A, et al. Choroidal changes in rhesus macaques in aging and age-related drusen. *Invest Ophthalmol Vis Sci*. 2023;64(12):44. https://doi.org/10.1167/iovs.64.12.44

Purpose. Choroidal vascular changes occur with normal aging and age-related macular degeneration (AMD). Here, we evaluate choroidal thickness and vascularity in aged rhesus macaques to better understand the choroid's role in this nonhuman primate model of AMD.

Methods. We analyzed optical coherence tomography (OCT) images of 244 eyes from 122 rhesus macaques (aged 4–32 years) to measure choroidal thickness (CT) and choroidal vascularity index (CVI). Drusen number, size, and volume were measured by semiautomated annotation and segmentation of OCT images. We performed regression analyses to determine any association of CT or CVI with age, sex, and axial length and to determine if the presence and volume of soft drusen impacted these choroidal parameters.

Results. In rhesus macaques, subfoveal CT decreased with age at 3.2 µm/y ($R^2 = 0.481$, $P < 0.001$), while CVI decreased at 0.66% per year ($R^2 = 0.257$, $P < 0.001$). Eyes with soft drusen exhibited thicker choroid (179.9 ± 17.5 µm vs. 162.0 ± 27.9 µm, $P < 0.001$) and higher CVI (0.612 ± 0.051 vs. 0.577 ± 0.093, $P = 0.005$) than age-matched control animals. Neither CT or CVI appeared to be associated with drusen number, size, or volume in this cohort. However, some drusen in macaques were associated with underlying choroidal vessel enlargement resembling pachydrusen in human patients with AMD.

Conclusions. Changes in the choroidal vasculature in rhesus macaques resemble choroidal changes in human aging, but eyes with drusen exhibit choroidal thickening, increased vascularity, and phenotypic characteristics of pachydrusen observed in some patients with AMD.

Keywords: choroid, aging, rhesus macaque, choroidal vascularity index, drusen

The aging eye is associated with a variety of degenerative ocular pathologies such as cataracts, glaucoma, and age-related macular degeneration (AMD).[1,2] AMD is the leading cause of irreversible blindness in individuals aged 50 years and older[1] and has been estimated to affect 288 million people worldwide by 2040.[3] The pathophysiology of AMD is complex and multifactorial, including oxidative stress, lipid peroxidation, complement dysregulation, and choroidal hypoperfusion.[4] The early stages of AMD are characterized by deposits known as soft drusen, which accumulate between the retinal pigment epithelium (RPE) and underlying Bruch's membrane located between the neurosensory retina and the choroidal vasculature. Later stages of AMD may include aberrant angiogenesis arising from the choroid known as choroidal neovascularization (CNV) and/or progressive degeneration of RPE, photoreceptors, and choroidal vessels causing geographic atrophy (GA). The intimate relationship between choroidal anatomy and AMD pathology warrants further understanding of the choroid's role in AMD pathophysiology.

The choroid is a highly vascular tissue consisting of membrane-lined lacunae, nonvascular smooth muscle cells, intrinsic choroidal neurons, melanocytes, and extracellular fluid within its stroma.[5] The choroid vasculature includes three layers—the outermost Haller's layer of large blood vessels, the Sattler's layer of medium-sized vessels, and the innermost choriocapillaris immediately adjacent to Bruch's membrane, which provides oxygen and nutrients to the overlying RPE and photoreceptors.[6] In humans, aging is associated with thinning of choroidal layers[7–10] and a reduction of choroidal vascularity—defined as the proportion of the luminal (vascular) versus stromal (interstitial) components of the choroid and expressed as the choroidal vascularity index (CVI).[8,10–17] Patients with AMD do not exhibit substantial changes in choroidal thickness (CT)[18] but have lower CVI, as seen on optical coherence tomography (OCT)

imaging.[19] A hemodynamic contribution to AMD pathogenesis has also been implicated by lower choriocapillaris density and other vascular changes measured using OCT angiography.[20–27]

Nonhuman primates (NHPs) such as rhesus macaques (*Macaca mulatta*) are ideal animal models of human aging. Rhesus monkeys age biologically at an approximate ratio of 3:1 as compared to humans, with puberty occurring between 2.5 and 4.5 years, menopause at 26 years, and a median life span of approximately 27 years.[28] These macaques during their third decade exhibit a decline in physical health, reduced physiologic integrity, and breakdown in muscle and brain functions that parallel human aging.[29,30] Epigenetic clocks developed based on genome methylation patterns also demonstrate cross-species conservation of biological aging mechanisms between humans and rhesus monkeys.[31] Importantly, unlike most laboratory animals, NHPs possess a cone-rich macula similar to that in humans[32–34] and spontaneously develop drusen lesions with old age.[35,36] NHP retinas with soft drusen exhibit histologic features of early AMD, as well as ultrastructural findings such as basal linear deposits (BLinD) and dome-shaped mounds of lipid particles under the RPE.[37] NHP drusen contents include vitronectin, apolipoprotein E, amyloid, and complement components C5 and C5b-9 complex.[36] Macaque eyes with drusen also exhibit reduced quantitative fundus autofluorescence (qAF) similar to human patients with AMD.[38] Interestingly, although NHP drusen undergo dynamic remodeling, including both progression and regression, NHP eyes do not develop geographic atrophy, choroidal neovascularization, or other signs of progression to advanced AMD.[37]

To better understand the role of choroidal anatomy in NHP aging and age-related drusen, we evaluated choroidal thickness and vascularity in a large cohort of rhesus macaques with normal eye exams, as well as aged animals with soft drusen identified on routine eye exams. Using OCT imaging to measure CT and CVI, we sought to determine if choroidal anatomy is impacted by age, sex, axial length, and presence or quantity of drusen lesions.

Methods

Clinical Examination

We performed ophthalmic examination of rhesus macaques (*M. mulatta*) between 4 and 32 years of age at the California National Primate Research Center (CNPRC). The examination protocols abided by the guidelines outlined by the ARVO Statement for the Use of Animals in Ophthalmic and Vision Research and the National Institutes of Health (NIH) guide for the Care and Use of Laboratory Animals. All procedures were approved by the University of California, Davis Institutional Animal Care and Use Committee. Macaques were sedated by intramuscular injection of ketamine hydrochloride, dexmedetomidine, and midazolam. Mydriasis was achieved with tropicamide (Bausch & Lomb, Tampa, FL, USA) and phenylephrine (Paragon Biosciences, Northbrook, IL, USA), and cycloplegia with cyclopentolate (Akorn, Lake Forest, IL, USA). Comprehensive ophthalmic examinations were performed by board-certified ophthalmologists (GY, AM) and a veterinary ophthalmologist (SMT), which included portable slit-lamp evaluation, indirect ophthalmoscopy, rebound tonometry (TovoVet; Icare, Vantaa, Finland), A-scan biometry to measure axial length (Sonomed 300A + PacScan Plus A-Scan; Carleton Optical, Buckinghamshire, UK), and external anterior segment photography (Rebel T3; Canon, Tokyo, Japan) as previously described.[39–41]

Ocular Imaging

Spectral-domain OCT images were obtained via the Spectralis HRA+OCT system (Heidelberg Engineering, Heidelberg, Germany) with a modified chinrest to accommodate the monkeys' facial contour. Animals underwent a 20° × 20° OCT volume scan with 1024 A-scans per B-scan and scan spacing of 25 µm, centered on the fovea in high-speed mode. We also captured 30° × 5° OCT raster scan with 1536 A-scans per B-scan and 234-μm spacing between B-scans in high-resolution enhanced-depth imaging mode. Twenty-five scans were averaged for each B-scan using eye-tracking automatic real-time software (Heidelberg Engineering). Only images with a signal strength of 6 or greater were utilized for the study. An artificial tear solution (GenTeal; Alcon, Geneva, Switzerland) was used to maintain the ocular surface. OCT images were obtained by GY at CNPRC, and the macaques were continuously monitored by a trained veterinary technician.

Choroidal Thickness and Vascularity Measurements

OCT images were exported from Heidelberg Explorer software (version 1.8.6.0; Heidelberg Engineering), and the subfoveal CT was measured from Bruch's membrane to the choroid–scleral junction (CSJ) by experienced masked graders (YS, AM, and EC) using the software caliper tool as previously described in human studies.[42–45] Choroidal vascularity parameters were measured using methods described by Sonoda et al.[12,13] and Agrawal et al.[11] Briefly, a 3-mm × 1-mm region centered on the fovea was cropped from the high-resolution enhanced-depth foveal OCT B-scan in ImageJ software (version 1.53; NIH, Bethesda, MD), and a subfoveal choroidal area with a horizontal width of 1,500 µm was manually selected as the region of interest[22] (Fig. 1A). Images were then binarized using the Niblack Auto Local Threshold technique, which accounts for the average and standard deviation[46] of all pixels within the region of interest (ROI) (Fig. 1B).[11,47] The luminal area (LA) and stromal area (SA) were measured from the black and white pixels, respectively, in the binarized ROI, which constitute the total choroidal area (TCA), and the CVI was computed as LA/TCA as previously defined.[11,47]

Drusen Size and Volume Measurements

Animals with soft drusen were identified from indirect ophthalmoscopy and fundus photography (Fig. 1C) and verified on OCT as dome-shaped sub-RPE deposits as previously reported.[35] Drusen number, size, and volume were determined from OCT images using the Duke Optical Coherence Tomography Retinal Analysis Program (DOCTRAP, version 62.0; Duke University, Durham, NC)[48–50] as described previously for both human and NHP studies.[35,37,38] Briefly, the RPE and Bruch's membrane were automatically segmented from OCT B-scan images, then manually adjusted by masked graders who also annotated the apex of each druse, defined as dome-shaped sub-RPE deposits on the OCT image (Figs. 1D, 1E). Drusen maps were generated by comput-

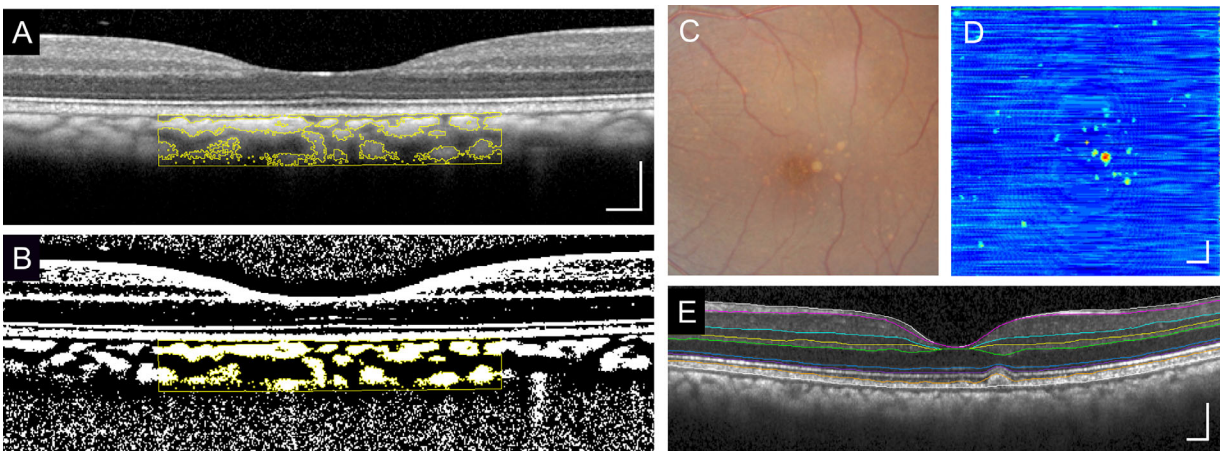

Figure 1. Measurement of choroidal thickness, choroidal vascularity, and drusen parameters. (**A**) Representative spectral-domain OCT B-scan image from a normal rhesus macaque eye and corresponding (**B**) binarized image performed using Niblack autolocal threshold with an overlay (*yellow outline*) of the binarized segment of the choroid within the subfoveal region of interest used to measure CT and CVI. (**C**) Representative color fundus photograph and (**D**) drusen map generated from the 20° × 20° OCT volume scan where (**E**) horizontal OCT B-scans were semiautomatically segmented to determine the RPE (*orange line*) and Bruch's membrane (*white line*) and each druse manually annotated to measure drusen number, average height, and volume. *Scale bars*: 200 µm.

ing the deviation of the segmented RPE layer from an approximation of the normal RPE without irregularities, obtained using polynomial fitting.[51–53] For each B-scan, the normal RPE was estimated by fitting a third-degree polynomial to the segmented RPE layer, after subtracting the vertical position of Bruch's membrane from the RPE to adjust for the curvature of the Bruch's membrane. The offset provided by the Bruch's membrane was then added back after fitting to obtain the resulting fitted RPE. Locations where the segmented RPE deviated from the fitted RPE by more than two standard deviations of the mean age-matched normative RPE-drusen complex (DC) thickness were used to generate drusen maps.[35] Since drusen are three-dimensional structures, polynomial fitting was also performed along the axis orthogonal to the OCT B-scans, and postprocessing of drusen maps was performed to remove spurious regions where RPE deviation only existed along a single axis. The generated drusen maps were used to determine the drusen volume within the central 5-mm circular region centered on the fovea, the average drusen height in that region, and the number of labeled drusen in this area (Fig. 1D).

Statistical Analysis

Statistical analyses were performed using SPSS software (version 22; IBM, Armonk, NY, USA). The association between choroidal parameters (CT, CVI, LA, SA, and TCA) with age, axial length, and drusen number, size, or volume was measured using univariate linear regression analyses with generalized estimating equations to account for two eyes measured per animal. Differences in CT and CVI between animals with drusen and age-matched control animals were assessed by independent samples Student's *t*-tests. All *P* values were two-sided and determined to be statistically significant when $P < 0.05$.

Results

Study Animals and Eyes

We analyzed 244 eyes of 122 animals with a mean age of 18.6 ± 6.8 years and 70% females. Mean axial length was 19.9 ± 0.7 mm. Soft drusen were noted in 28 eyes of 14 animals, which occurred primarily among older animals (age range, 16.6–29.2) as expected, given the increased prevalence of this feature with age. Among eyes with drusen, the mean number of lesions was 22.8 ± 18.6 per eye, mean drusen height was 10.0 ± 6.4 µm, and mean drusen volume was 0.070 ± 0.068 mm^3. These values are comparable to our previous studies of drusen dimensions in rhesus macaques[35] and consistent with those in human patients with AMD.[54,55]

Choroidal Thickness in NHP Aging and Drusen

Subfoveal CT varied among individual animals with a mean value of 179.6 ± 30.4 µm, which is similar to normative values reported in a smaller cohort of rhesus macaques (191.2 ± 43.0 µm) and slightly lower than CT in humans (266.8 ± 78.0 µm).[56,57] CT in macaque eyes decreased linearly with age at 3.1 µm/y ($\beta = 0.047$, $P < 0.001$, Fig. 2A), which is comparable to the rate of choroidal thinning in humans at 2.98 µm/y.[58] Female animals had thinner choroid than male counterparts (mean 173.2 ± 29.0 µm vs. 193.0 ± 29.2 µm, β = 3.84E8, $P < 0.001$, Fig. 2B), as observed in humans.[57,59] However, subfoveal CT in our cohort did not vary with axial length ($\beta = 1.59$, $P = 0.798$, Fig. 2C), as previously noted in humans.[57,60,61] Interestingly, NHP eyes with soft drusen appeared to have thicker choroids compared to age-matched control animals (179.9 ± 17.5 µm vs. 162.0 ± 27.9 µm, $P < 0.001$) or to the entire normal cohort when adjusted for age (β = 3.13E-09, $P < 0.001$, Fig. 2A), which contrasts with typical patients with AMD.[62]

Choroidal Vascularity in NHP Aging and Drusen

Mean CVI in our cohort of macaques was 0.589 ± 0.088, which also decreased with age at a rate of 0.66% per year ($\beta = 0.993$, $P < 0.001$, Fig. 2D), similar to age-related CVI changes in humans.[14] The decline in choroidal vascularity appears to be mainly caused by a reduction in luminal rather than stromal components, as LA decreases more rapidly than SA or TCA with age (Supplementary Fig. S1). Mean CVI was also greater in males than females (0.62 vs. 0.57, $\beta = 1.046$, $P = 0.002$, Fig. 2E), but showed no relationship with axial

Investigative Ophthalmology & Visual Science

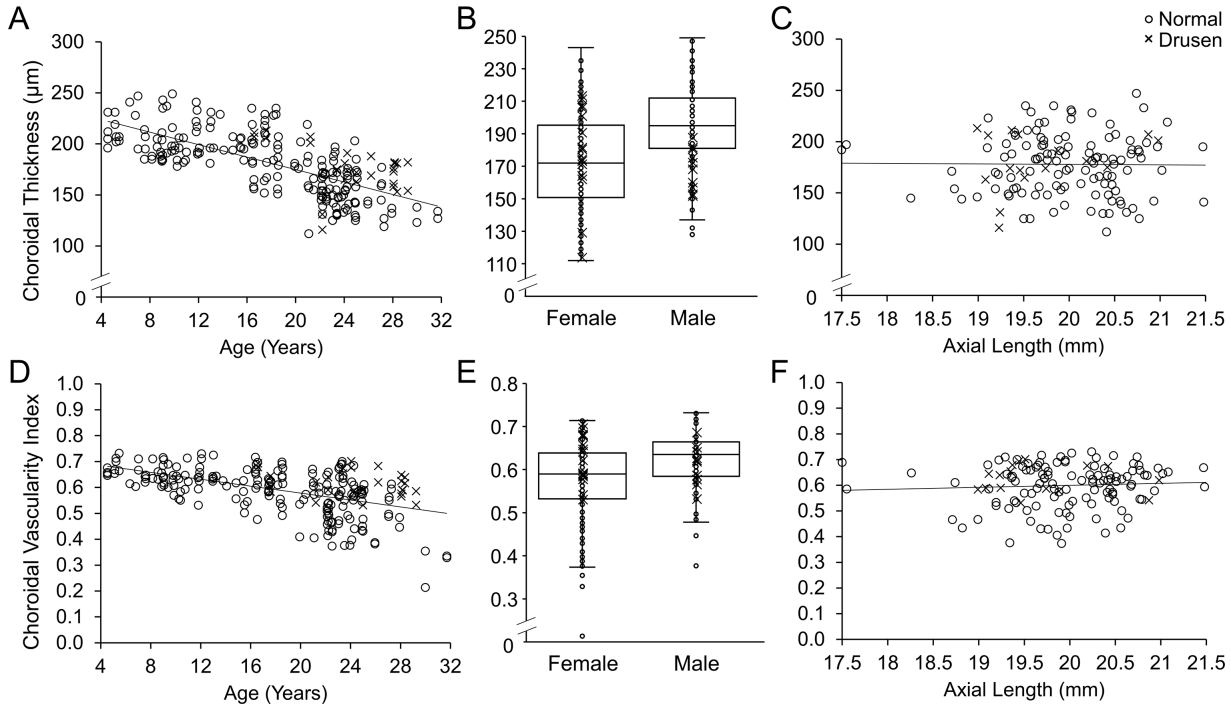

Figure 2. Relationship of choroidal thickness and vascularity with age, sex, and axial length. Scatterplots and box-and-whisker plots showing the relationship of (**A–C**) subfoveal choroidal thickness and (**D–F**) choroidal vascularity index with age (**A**, **D**), sex (**B**, **E**), and axial length (**C**, **F**), with regression trend lines and comparing eyes with drusen (*crossmarks*) or normal eyes (*circles*).

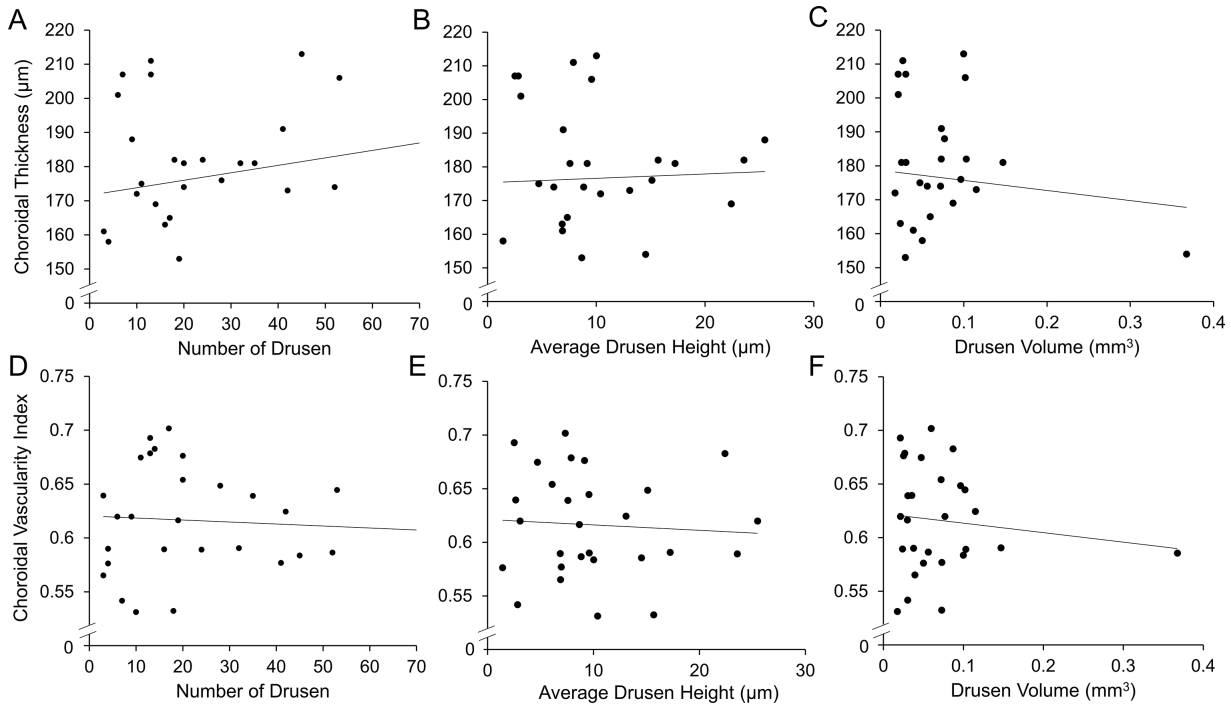

Figure 3. Relationship of choroidal thickness and vascularity with drusen parameters. Scatterplots showing the relationship between (**A–C**) subfoveal choroidal thickness and (**D–F**) choroidal vascularity index with number of drusen (**A**, **D**), average drusen height (**B**, **E**), and drusen volume (**C**, **F**) for each eye, with regression trend line.

length ($\beta = 1.004$, $P = 0.447$, Fig. 2F). Similar to choroidal thickness, we found that choroidal vascularity was greater in animals with soft drusen compared with age-matched control animals (0.612 ± 0.051 vs. 0.577 ± 0.093, $P = 0.005$) or when compared with the normal cohort and adjusted for age ($\beta = 0.917$, $P < 0.001$, Fig. 2D). Our findings differ

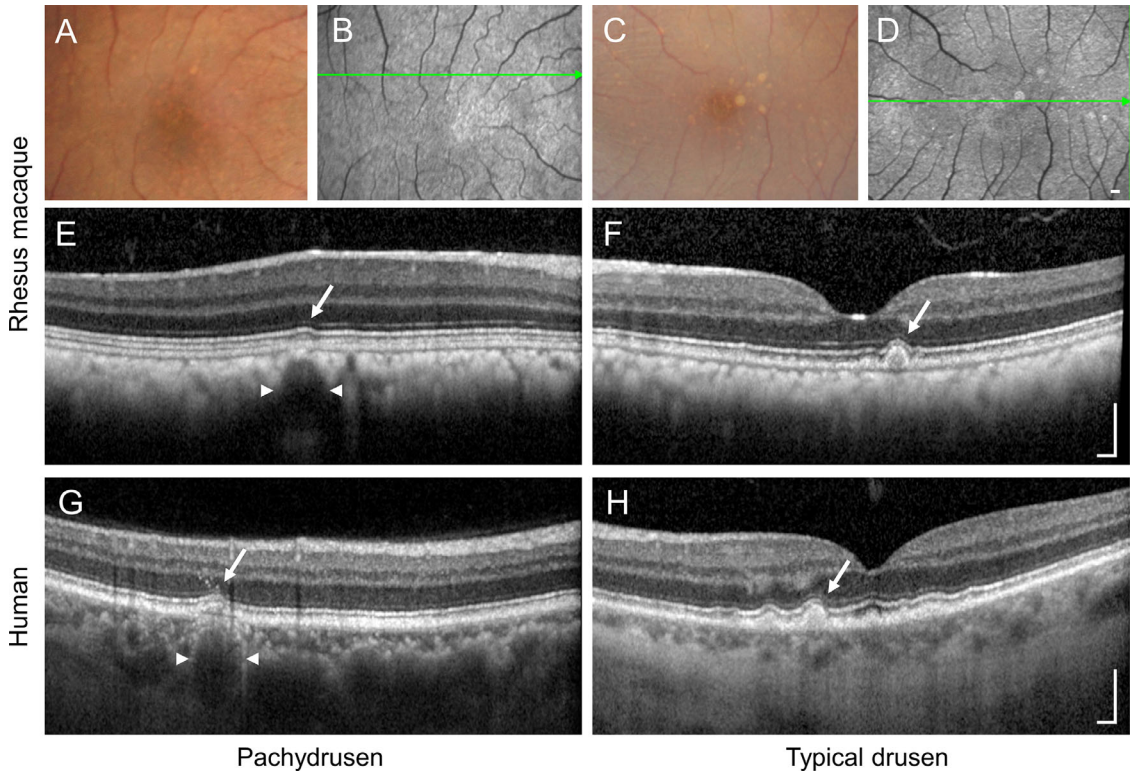

Figure 4. Pachydrusen versus typical drusen phenotypes in macaques and human AMD. Representative (**A**, **C**) color fundus photographs and (**B**, **D**) fundus autofluorescence images with (**E–H**) spectral-domain OCT B-scans of eyes with drusen from rhesus macaques (**A–F**) and human patients with AMD (**G–H**) that exhibit the pachydrusen phenotype (**A**, **B**, **E**, **G**) where the drusen (*arrow*) overlie large-caliber choroidal vessels (*arrowheads*) versus more typical drusen phenotype (**C**, **D**, **F**, **H**). The macaque OCT B-scans in (**E**) and (**F**) correspond to the *green arrow* in (**B**) and (**D**). Images from human subjects were obtained from patients seen at the University of California, Davis Health system. Scale bars: 200 µm.

from those observed in human patients with AMD, in whom choroidal vascularity appears to be decreased in eyes with drusen.[63]

Choroidal Parameters and Drusen Severity

To better understand the relationship between choroidal anatomy and NHP drusen, we searched for an association between choroidal thickness or vascularity and drusen number, size, or volume in the aged macaques that exhibited these AMD-like lesions. We found that neither CT nor CVI appeared to be associated with drusen number, size, or volume (P = 0.517–0.845 for CT and P = 0.309–0.755 for CVI, Figs. 3A–F) in this cohort of rhesus macaques with drusen, although there was a slight trend toward thicker choroid among eyes with more drusen.

Choroidal Pachyvessels Underlie Some NHP Drusen

Close fundus examination of the drusen phenotype in rhesus macaques revealed that most drusen demonstrated discrete borders and occurred in isolation rather than in confluent clusters (Figs. 4A, 4B). Some lesions appeared to directly overlie the hyporeflective lumen of large choroidal vessels on OCT imaging (Fig 4E), although more typical drusen in these animals did not show clear underlying choroidal changes (Figs. 4C, 4D, 4F). These features are reminiscent of the "pachydrusen" phenotype in subsets of human patients with AMD, which are associated with thickened choroid (Fig. 4G), in contrast to more typical-appearing drusen where the choroid is thinner (Fig. 4H).[64]

Discussion

The choroid of the eye is the primary vascular supply to the outer retina but also can modulate the retinal focal plane and regulate eye growth among many other functions.[5] Choroidal hypoperfusion has been implicated in the pathogenesis of AMD, although its specific impact is unclear. To better understand the choroid's role in aging and AMD, we explored choroidal thickness and vascularity using live ocular imaging in a large cohort of aging rhesus macaques, including those that exhibit drusen. Nonhuman primates are uniquely suited to serve as animal models of AMD because they possess a cone-rich macula resembling humans and spontaneously develop drusen—the hallmark feature of AMD. Soft drusen in macaques undergo similar patterns of remodeling and progression[35,37] and have similar histologic, ultrastructural, and molecular characteristics as human drusen.[36,37] In this study, we found that older age and female sex are associated with choroidal thinning and loss of vascularity, similar to humans. However, we also found that macaque eyes with drusen have thicker choroid and greater vascularity, in contrast to most human eyes with typical AMD, and resemble the "pachydrusen" appearance observed in subsets of patients with AMD.[65] Our findings

provide insight into the similarities and differences between NHP drusen and human AMD, as well as the impact of the choroid in drusen pathobiology.

Previous studies have implicated the choroid's role in the pathogenesis of AMD, based on changes in choroidal thickness, choroidal vascularity, and choriocapillaris flow density as seen on OCT and OCT angiography.[18–23] However, these findings were often confounded by the heterogeneity of AMD phenotypes, varying degrees of AMD severity, and the choroidal thinning that occurs with normal aging in humans. For example, while early studies suggested that choroidal thinning occurs with greater AMD severity, these differences were no longer observed when adjusted for age.[18] Instead, choroidal thinning appears to occur only in eyes with specific AMD features such as reticular pseudodrusen or geographic atrophy, rather than drusen alone.[66,67] The choroid also appears thicker in eyes with CNV,[68,69] although choroidal vascularity is reduced in both nonexudative and exudative AMD, presumably attributed to increased inflammatory infiltrates in the choroid stroma.[70] Unlike human AMD, macaques with drusen do not exhibit reticular pseudodrusen and do not progress to CNV or GA. NHP drusen also do not demonstrate hyperreflective foci, hyporeflective cores, drusen substructures, or other OCT biomarkers or predictors of GA progression in humans.[71–74] Although soft drusen in macaques resemble those in patients with AMD in anatomy and molecular composition, the overlying RPE and photoreceptors do not show degenerative changes on histology or quantitative autofluorescence.[37,38] Instead, our current study suggests that NHP drusen are associated with thicker choroid and greater vascularity, resembling pachydrusen rather than typical soft drusen in AMD.

The term *pachydrusen* was coined by Richard Spaide due to distinctive clinical characteristics such as larger size, irregular contour, scattered distribution, and frequent occurrence in isolation.[64] Importantly, drusen with these features were associated with eyes with thicker choroid, also known as pachychoroid. The pathogenesis of pachydrusen is unclear, although the anatomic appearance on OCT (Figs. 4E, 4G) suggests focal compression of the choriocapillaris by the underlying enlarged choroidal vessel ("pachyvessel") impairing choriocapillary outflow and resulting in sub-RPE deposits. Other pachychoroid retinal diseases, which include central serous chorioretinopathy and polypoidal choroidal vasculopathy, are associated with pachyvessels and hyperpermeability, with increased choroidal thickness and vascularity.[75,76] This spectrum of conditions overlaps with features seen in AMD but has distinct racial dispositions. In contrast to white or Caucasian patients, Asians are more likely to have pachychoroid diseases and exhibit pachydrusen with thicker, more vascular choroids and less likely to have typical AMD or reticular pseudodrusen, which are associated with choroidal thinning and decreased CVI.[77] Genome-wide association studies (GWASs) have identified susceptibility loci for pachychoroid diseases in *CFH*, *VIPR2*, *TNFRSF10A*, and near *GATA5* from both Japanese and European cohorts,[78,79] among which *CFH* and *TFRSF10A* have been identified from GWASs of more typical patients with AMD from the International AMD Genomics Consortium.[80] Beside differences in genetic background, Asians also exhibit darker ocular pigmentation, similar to the darker uveal pigment in rhesus macaques.[56] Melanin participates in filtering ultraviolet radiation and scavenging reactive oxygen species and may have a protective effect against oxidative damage that contributes to RPE injury and GA. Finally, despite the parallels between the biological life span of macaques and humans, including development, maturation, reproduction, and aging, the chronological age of these NHPs is considerably shorter. Monkeys in captivity may also demonstrate less genetic background heterogeneity,[81] healthier diets, and less severe environmental exposures than free-ranging animals or humans.[82] Thus, the drusen phenotype in our NHP cohort may reflect differences in genetic background, uveal pigmentation, chronological age, and dietary and environmental factors as compared to humans.

In addition to providing insight into drusen pathophysiology in NHPs versus humans, our study also provided normative values of CT and CVI in healthy rhesus macaques across their life span. We observed age-related choroidal thinning and loss of vascularity, as well as sex-related differences that are similar to trends observed in humans.[9,59] We did not observe significant association with axial length, unlike human studies that showed choroidal thinning in more myopic eyes.[57] We hypothesize this is due to the narrow range of axial lengths and low frequency of highly myopic eyes seen in our cohort. Our team recently identified an animal with high myopia, axial elongation, and myopic foveoschisis that did demonstrate choroidal thinning.[83]

Limitations of our study include the cross-sectional nature of our analysis and the absence of longitudinal data afforded by a cohort design that would have required significantly more time. Also, a potential challenge for measuring choroidal thickness and vascularity in macaques stems from the darker uveal pigmentation, which increases light scatter on spectral-domain OCT imaging and reduces the clear delineation of the CSJ.[42,56] However, given that CT in NHPs has been evaluated in other studies[84] and that our data closely follow trends from human studies, we believe that the large sample size in our study helps to increase the reproducibility of CT or CVI measurements. Additional strengths of our study include the use of masked graders and semiautomated segmentation of drusen to provide more robust, quantitative analysis of the drusen phenotype.

In summary, our study revealed gradual age-related thinning and loss of vascularity in the choroid of rhesus macaques, similar to humans, but found that eyes with NHP drusen had thicker choroid and greater vascularity, with a phenotype resembling pachydrusen that are found in unique subsets of patients with AMD. Future studies to explore the cellular and molecular contributions to drusen biogenesis in these animals, as well as their genetic associations, could help further determine the utility of NHP as a model of AMD.

Acknowledgments

The authors thank Monica Motta, Jae Ho Shim, Brett Donald Story, Sophie Le, and Michele Ferneding for assistance with animal imaging; Connie Fountain, Mary Roberts, and Paul-Michael Sosa for rhesus macaque colony management; and Jeffrey A. Roberts and John Morrison for CNPRC support.

Supported by the Office of Research Infrastructure Program/OD (P510D011107; CNPRC) and the large animal imaging core of NEI P30 EY12576. GY is supported by NIH R01 EY032238, R21 EY031108, Foundation Fighting Blindness, the BrightFocus Foundation, US Department of Agriculture, and University of California Office of the President. SMT and AM are supported by NIH U24 EY029904. SF is supported by P30 EY005722. No funding organizations had any role in the design or conduct of this research. The content is solely the responsibility of the

authors and does not necessarily represent the official views of the funding agencies.

Disclosure: **Y. Sazhnyev**, None; **T.-N. Sin**, None; **A. Ma**, None; **E. Chang**, None; **L. Huynh**, None; **K. Roszak**, None; **S. Park**, None; **K. Choy**, None; **S. Farsiu**, None; **A. Moshiri**, None; **S.M. Thomasy**, None; **G. Yiu**, Abbvie (C), Adverum (C), Alimera (C), Bausch & Lomb (C), Clearside (C), Endogena (C), Genentech (C), Gyroscope (C), Intergalactic (C), Iridex (C), Janssen (C), Myro (C), NGM Biopharmaceutical (C), Novartis (C), Regeneron (C), Thea (C), Topcon (C), Zeiss (C)

References

1. Flaxman SR, Bourne RRA, Resnikoff S, et al. Global causes of blindness and distance vision impairment 1990-2020: a systematic review and meta-analysis. *Lancet Glob Health*. 2017;5:e1221–e1234.
2. Li Z, Hu Y, Yu H, Li J, Yang X. Effect of age and refractive error on quick contrast sensitivity function in Chinese adults: a pilot study. *Eye (Lond)*. 2021;35:966–972.
3. Wong WL, Su X, Li X, et al. Global prevalence of age-related macular degeneration and disease burden projection for 2020 and 2040: a systematic review and meta-analysis. *Lancet Glob Health*. 2014;2:e106–e116.
4. Seddon JM, McLeod DS, Bhutto IA, et al. Histopathological insights into choroidal vascular loss in clinically documented cases of age-related macular degeneration. *JAMA Ophthalmol*. 2016;134:1272–1280.
5. Nickla DL, Wallman J. The multifunctional choroid. *Prog Retin Eye Res*. 2010;29:144–168.
6. Edwards M, Lutty GA. Bruch's membrane and the choroid in age-related macular degeneration. *Adv Exp Med Biol*. 2021;1256:89–119.
7. Adhi M, Ferrara D, Mullins RF, et al. Characterization of choroidal layers in normal aging eyes using enface swept-source optical coherence tomography. *PLoS One*. 2015;10:e0133080.
8. Tuncer I, Karahan E, Zengin MO, Atalay E, Polat N. Choroidal thickness in relation to sex, age, refractive error, and axial length in healthy Turkish subjects. *Int Ophthalmol*. 2015;35:403–410.
9. Wei WB, Xu L, Jonas JB, et al. Subfoveal choroidal thickness: the Beijing Eye Study. *Ophthalmology*. 2013;120:175–180.
10. Ikuno Y, Kawaguchi K, Nouchi T, Yasuno Y. Choroidal thickness in healthy Japanese subjects. *Invest Ophthalmol Vis Sci*. 2010;51:2173–2176.
11. Agrawal R, Gupta P, Tan KA, Cheung CM, Wong TY, Cheng CY. Choroidal vascularity index as a measure of vascular status of the choroid: measurements in healthy eyes from a population-based study. *Sci Rep*. 2016;6:21090.
12. Sonoda S, Sakamoto T, Yamashita T, et al. Choroidal structure in normal eyes and after photodynamic therapy determined by binarization of optical coherence tomographic images. *Invest Ophthalmol Vis Sci*. 2014;55:3893–3899.
13. Sonoda S, Sakamoto T, Yamashita T, et al. Luminal and stromal areas of choroid determined by binarization method of optical coherence tomographic images. *Am J Ophthalmol*. 2015;159:1123–1131.e1121.
14. Nivison-Smith L, Khandelwal N, Tong J, Mahajan S, Kalloniatis M, Agrawal R. Normal aging changes in the choroidal angioarchitecture of the macula. *Sci Rep*. 2020;10:10810.
15. Eriş E. Association between choroidal vascular density, age and sex: a prospective study. *Photodiagnosis Photodyn Ther*. 2019;27:452–454.
16. Zhou H, Dai Y, Shi Y, et al. Age-related changes in choroidal thickness and the volume of vessels and stroma using swept-source OCT and fully automated algorithms. *Ophthalmol Retina*. 2020;4:204–215.
17. Barteselli G, Chhablani J, El-Emam S, et al. Choroidal volume variations with age, axial length, and sex in healthy subjects: a three-dimensional analysis. *Ophthalmology*. 2012;119:2572–2578.
18. Yiu G, Chiu SJ, Petrou PA, et al. Relationship of central choroidal thickness with age-related macular degeneration status. *Am J Ophthalmol*. 2015;159:617–626.
19. Koh LHL, Agrawal R, Khandelwal N, Sai Charan L, Chhablani J. Choroidal vascular changes in age-related macular degeneration. *Acta Ophthalmol*. 2017;95:e597–e601.
20. Rosenfeld PJ, Trivizki O, Gregori G, Wang RK. An update on the hemodynamic model of age-related macular degeneration. *Am J Ophthalmol*. 2022;235:291–299.
21. Zheng F, Zhang Q, Shi Y, et al. Age-dependent changes in the macular choriocapillaris of normal eyes imaged with swept-source optical coherence tomography angiography. *Am J Ophthalmol*. 2019;200:110–122.
22. Roisman L, Zhang Q, Wang RK, et al. Optical coherence tomography angiography of asymptomatic neovascularization in intermediate age-related macular degeneration. *Ophthalmology*. 2016;123:1309–1319.
23. Palejwala NV, Jia Y, Gao SS, et al. Detection of nonexudative choroidal neovascularization in age-related macular degeneration with optical coherence tomography angiography. *Retina*. 2015;35:2204–2211.
24. Lee SC, Rusakevich AM, Amin A, et al. Long-term retinal vascular changes in age-related macular degeneration measured using optical coherence tomography angiography. *Ophthalmic Surg Lasers Imaging Retina*. 2022;53:529–536.
25. Lee SC, Tran S, Amin A, et al. Retinal vessel density in exudative and nonexudative age-related macular degeneration on optical coherence tomography angiography. *Am J Ophthalmol*. 2020;212:7–16.
26. Snyder K, Yazdanyar A, Mahajan A, Yiu G. Association between the cilioretinal artery and choroidal neovascularization in age-related macular degeneration: a secondary analysis from the Age-Related Eye Disease Study. *JAMA Ophthalmol*. 2018;136:1008–1014.
27. Toulouie S, Chang S, Pan J, Snyder K, Yiu G. Relationship of retinal vessel caliber with age-related macular degeneration. *J Ophthalmol*. 2022;2022:8210599.
28. Simmons HA. Age-associated pathology in rhesus macaques (Macaca mulatta). *Vet Pathol*. 2016;53:399–416.
29. Roth GS, Mattison JA, Ottinger MA, Chachich ME, Lane MA, Ingram DK. Aging in rhesus monkeys: relevance to human health interventions. *Science*. 2004;305:1423–1426.
30. Chiou KL, Montague MJ, Goldman EA, et al. Rhesus macaques as a tractable physiological model of human ageing. *Philos Trans R Soc Lond B Biol Sci*. 2020;375:20190612.
31. Horvath S, Zoller JA, Haghani A, et al. Epigenetic clock and methylation studies in the rhesus macaque. *Geroscience*. 2021;43:2441–2453.
32. Hendrickson A, Zhang C. Development of cone photoreceptors and their synapses in the human and monkey fovea. *J Comp Neurol*. 2019;527:38–51.
33. Francis PJ, Appukuttan B, Simmons E, et al. Rhesus monkeys and humans share common susceptibility genes for age-related macular disease. *Hum Mol Genet*. 2008;17:2673–2680.
34. Cornish EE, Madigan MC, Natoli R, Hales A, Hendrickson AE, Provis JM. Gradients of cone differentiation and FGF expression during development of the foveal depression in macaque retina. *Vis Neurosci*. 2005;22:447–459.

35. Yiu G, Tieu E, Munevar C, et al. In vivo multimodal imaging of drusenoid lesions in rhesus macaques. *Sci Rep*. 2017;7:15013.
36. Umeda S, Suzuki MT, Okamoto H, et al. Molecular composition of drusen and possible involvement of anti-retinal autoimmunity in two different forms of macular degeneration in cynomolgus monkey (Macaca fascicularis). *FASEB J*. 2005;19:1683–1685.
37. Yiu G, Chung SH, Mollhoff IN, et al. Long-term evolution and remodeling of soft drusen in rhesus macaques. *Invest Ophthalmol Vis Sci*. 2020;61:32.
38. Tran TM, Kim S, Lin KH, et al. Quantitative fundus autofluorescence in rhesus macaques in aging and age-related drusen. *Invest Ophthalmol Vis Sci*. 2020;61:16.
39. Lin KH, Tran T, Kim S, et al. Age-related changes in the rhesus macaque eye. *Exp Eye Res*. 2021;212:108754.
40. Lin KH, Tran T, Kim S, et al. Advanced retinal imaging and ocular parameters of the rhesus macaque eye. *Transl Vis Sci Technol*. 2021;10:7.
41. Chung SH, Mollhoff IN, Mishra A, et al. Host immune responses after suprachoroidal delivery of AAV8 in nonhuman primate eyes. *Hum Gene Ther*. 2021;32:682–693.
42. Yiu G, Pecen P, Sarin N, et al. Characterization of the choroid-scleral junction and suprachoroidal layer in healthy individuals on enhanced-depth imaging optical coherence tomography. *JAMA Ophthalmol*. 2014;132:174–181.
43. Vuong VS, Moisseiev E, Cunefare D, Farsiu S, Moshiri A, Yiu G. Repeatability of choroidal thickness measurements on enhanced depth imaging optical coherence tomography using different posterior boundaries. *Am J Ophthalmol*. 2016;169:104–112.
44. Yiu G, Wang Z, Munevar C, et al. Comparison of chorioretinal layers in rhesus macaques using spectral-domain optical coherence tomography and high-resolution histological sections. *Exp Eye Res*. 2018;168:69–76.
45. Wong SS, Vuong VS, Cunefare D, Farsiu S, Moshiri A, Yiu G. Macular fluid reduces reproducibility of choroidal thickness measurements on enhanced depth optical coherence tomography. *Am J Ophthalmol*. 2017;184:108–114.
46. Tolun G, Vijayasarathy C, Huang R, et al. Paired octamer rings of retinoschisin suggest a junctional model for cell–cell adhesion in the retina. *Proc Natl Acad Sci USA*. 2016;113:5287–5292.
47. Yiu G, Vuong VS, Tran S, et al. Vascular response to sildenafil citrate in aging and age-related macular degeneration. *Sci Rep*. 2019;9:5049.
48. Farsiu S, Chiu SJ, O'Connell RV, et al. Quantitative classification of eyes with and without intermediate age-related macular degeneration using optical coherence tomography. *Ophthalmology*. 2014;121:162–172.
49. Chiu SJ, Toth CA, Bowes Rickman C, Izatt JA, Farsiu S. Automatic segmentation of closed-contour features in ophthalmic images using graph theory and dynamic programming. *Biomed Opt Express*. 2012;3:1127–1140.
50. Chiu SJ, Li XT, Nicholas P, Toth CA, Izatt JA, Farsiu S. Automatic segmentation of seven retinal layers in SDOCT images congruent with expert manual segmentation. *Opt Express*. 2010;18:19413–19428.
51. Chen Q, Leng T, Zheng L, et al. Automated drusen segmentation and quantification in SD-OCT images. *Med Image Anal*. 2013;17:1058–1072.
52. Farsiu S CS, Izatt JA, Toth CA. Fast detection and segmentation of drusen in retinal optical coherence tomography images. In: Stuck BE, Belkin M, Manns F, Söderberg PG, Ho A, eds. *Proceedings Volume 6844, Ophthalmic Technologies XVIII*. San Jose, California, USA: SPIE BiOS, 2008 Digital Library; 2008:68440D.
53. Zadeh GZ, Wintergerst MWM, Wiens V, et al. CNNs enable accurate and fast segmentation of drusen in optical coherence tomography. In: Jorge Cardoso M, Arbel T, Carneiro G, et al., eds. *Deep Learning in Medical Image Analysis and Multimodal Learning for Clinical Decision Support*. Québec City, QC, Canada: Springer, Cham; 2017:65–73.
54. Waldstein SM, Vogl WD, Bogunovic H, Sadeghipour A, Riedl S, Schmidt-Erfurth U. Characterization of drusen and hyperreflective foci as biomarkers for disease progression in age-related macular degeneration using artificial intelligence in optical coherence tomography. *JAMA Ophthalmol*. 2020;138:740–747.
55. Corvi F, Srinivas S, Nittala MG, et al. Reproducibility of qualitative assessment of drusen volume in eyes with age related macular degeneration. *Eye (Lond)*. 2021;35:2594–2600.
56. Yiu G, Vuong VS, Oltjen S, et al. Effect of uveal melanocytes on choroidal morphology in rhesus macaques and humans on enhanced-depth imaging optical coherence tomography. *Invest Ophthalmol Vis Sci*. 2016;57:5764–5771.
57. Goldenberg D, Moisseiev E, Goldstein M, Loewenstein A, Barak A. Enhanced depth imaging optical coherence tomography: choroidal thickness and correlations with age, refractive error, and axial length. *Ophthalmic Surg Lasers Imaging*. 2012;43:296–301.
58. Wakatsuki Y, Shinojima A, Kawamura A, Yuzawa M. Correlation of aging and segmental choroidal thickness measurement using swept source optical coherence tomography in healthy eyes. *PLoS One*. 2015;10:e0144156.
59. Li XQ, Larsen M, Munch IC. Subfoveal choroidal thickness in relation to sex and axial length in 93 Danish university students. *Invest Ophthalmol Vis Sci*. 2011;52:8438–8441.
60. Abbey AM, Kuriyan AE, Modi YS, et al. Optical coherence tomography measurements of choroidal thickness in healthy eyes: correlation with age and axial length. *Ophthalmic Surg Lasers Imaging Retina*. 2015;46:18–24.
61. Zhao J, Wang YX, Zhang Q, Wei WB, Xu L, Jonas JB. Macular choroidal small-vessel layer, Sattler's layer and Haller's layer thicknesses: the Beijing Eye Study. *Sci Rep*. 2018;8:4411.
62. Sigler EJ, Randolph JC. Comparison of macular choroidal thickness among patients older than age 65 with early atrophic age-related macular degeneration and normals. *Invest Ophthalmol Vis Sci*. 2013;54:6307–6313.
63. Sacconi R, Vella G, Battista M, et al. Choroidal vascularity index in different cohorts of dry age-related macular degeneration. *Transl Vis Sci Technol*. 2021;10:26.
64. Spaide RF. Disease expression in nonexudative age-related macular degeneration varies with choroidal thickness. *Retina*. 2018;38:708–716.
65. Zhang X, Sivaprasad S. Drusen and pachydrusen: the definition, pathogenesis, and clinical significance. *Eye (Lond)*. 2021;35:121–133.
66. Adhi M, Lau M, Liang MC, Waheed NK, Duker JS. Analysis of the thickness and vascular layers of the choroid in eyes with geographic atrophy using spectral-domain optical coherence tomography. *Retina*. 2014;34:306–312.
67. Capuano V, Souied EH, Miere A, Jung C, Costanzo E, Querques G. Choroidal maps in non-exudative age-related macular degeneration. *Br J Ophthalmol*. 2016;100:677–682.
68. Grunwald JE, Hariprasad SM, DuPont J, et al. Foveolar choroidal blood flow in age-related macular degeneration. *Invest Ophthalmol Vis Sci*. 1998;39:385–390.
69. Noori J, Riazi Esfahani M, Hajizadeh F, Zaferani MM. Choroidal mapping; a novel approach for evaluating choroidal thickness and volume. *J Ophthalmic Vis Res*. 2012;7:180–185.
70. Krytkowska E, Grabowicz A, Mozolewska-Piotrowska K, Ulańczyk Z, Safranow K, Machalińska A. The impact of

Investigative Ophthalmology & Visual Science

vascular risk factors on the thickness and volume of the choroid in AMD patients. *Sci Rep*. 2021;11:15106.

71. Christenbury JG, Folgar FA, O'Connell RV, et al. Progression of intermediate age-related macular degeneration with proliferation and inner retinal migration of hyperreflective foci. *Ophthalmology*. 2013;120:1038–1045.
72. Folgar FA, Chow JH, Farsiu S, et al. Spatial correlation between hyperpigmentary changes on color fundus photography and hyperreflective foci on SDOCT in intermediate AMD. *Invest Ophthalmol Vis Sci*. 2012;53:4626–4633.
73. Nassisi M, Fan W, Shi Y, et al. Quantity of intraretinal hyperreflective foci in patients with intermediate age-related macular degeneration correlates with 1-year progression. *Invest Ophthalmol Vis Sci*.. 2018;59:3431–3439.
74. Veerappan M, El-Hage-Sleiman AM, Tai V, et al. Optical coherence tomography reflective drusen substructures predict progression to geographic atrophy in age-related macular degeneration. *Ophthalmology*. 2016;123:2554–2570.
75. Xu D, Garg E, Lee K, et al. Long-term visual and anatomic outcomes of patients with peripapillary pachychoroid syndrome. *Br J Ophthalmol*. 2022;106:576–581.
76. Sakurada Y, Leong BCS, Parikh R, Fragiotta S, Freund KB. Association between choroidal caverns and choroidal vascular hyperpermeability in eyes with pachychoroid diseases. *Retina*. 2018;38:1977–1983.
77. Cheung CMG, Gan A, Yanagi Y, Wong TY, Spaide R. Association between choroidal thickness and drusen subtypes in age-related macular degeneration. *Ophthalmol Retina*. 2018;2:1196–1205.
78. Hosoda Y, Miyake M, Schellevis RL, et al. Genome-wide association analyses identify two susceptibility loci for pachychoroid disease central serous chorioretinopathy. *Commun Biol*. 2019;2:468.
79. Hosoda Y, Yoshikawa M, Miyake M, et al. CFH and VIPR2 as susceptibility loci in choroidal thickness and pachychoroid disease central serous chorioretinopathy. *Proc Natl Acad Sci USA*. 2018;115:6261–6266.
80. Fritsche LG, Igl W, Bailey JN, et al. A large genome-wide association study of age-related macular degeneration highlights contributions of rare and common variants. *Nat Genet*. 2016;48:134–143.
81. Ng J, Trask JS, Smith DG, Kanthaswamy S. Heterospecific SNP diversity in humans and rhesus macaque (Macaca mulatta). *J Med Primatol*. 2015;44:194–201.
82. Smit-McBride Z, Nguyen J, Elliott GW, et al. Effects of aging and environmental tobacco smoke exposure on ocular and plasma circulatory microRNAs in the Rhesus macaque. *Mol Vis*. 2018;24:633–646.
83. Sin TN, Kim S, Li Y, et al. A spontaneous nonhuman primate model of myopic foveoschisis. *Invest Ophthalmol Vis Sci*. 2023;64:18.
84. Cheong KX, Barathi VA, Teo KYC, et al. Choroidal and retinal changes after systemic adrenaline and photodynamic therapy in non-human primates. *Invest Ophthalmol Vis Sci*. 2021;62:25.